Available online at www.sciencedirect.com
ScienceDirect
Nuclear Physics A 837 (2010) 163–175
NUCLEAR PHYSICS A
www.elsevier.com/locate/nuclphysa

Statistical and dynamical aspects in the decay of hot neutron-rich nuclei

M. Veselsky [a,c], G.A. Souliotis [b,c,*], A.L. Keksis [c,1], M. Jandel [c,1], D.V. Shetty [c,2], S.J. Yennello [c], K. Wang [d], Y.G. Ma [d]

[a] *Institute of Physics, Slovak Academy of Sciences, Dubravska cesta 9, 84511 Bratislava, Slovakia*
[b] *Laboratory of Physical Chemistry, Department of Chemistry, National and Kapodistrian University of Athens, Panepistimiopolis, Athens 15771, Greece*
[c] *Cyclotron Institute, Texas A&M University, College Station, TX 77843, USA*
[d] *Shanghai Institute of Applied Physics, Shanghai, China*

Received 28 October 2009; received in revised form 29 January 2010; accepted 25 February 2010

Available online 10 March 2010

Abstract

A signal of isospin-asymmetric phase transition in the evolution of the chemical potential was observed in hot quasi-projectiles produced in the reactions ^{40,48}Ca + ^{27}Al confirming an analogous observation in the lighter quasi-projectiles observed in the reaction ^{28}Si + ^{112,124}Sn (Veselsky et al., 2004 [1]). With increasing mass, the properties of hot quasi-projectiles become increasingly influenced by secondary emission. Thermodynamical observables exhibit no sensitivity to the different number of missing (undetected) neutrons in the two reactions ^{40,48}Ca + ^{27}Al and provide a signal of dynamical emission of neutrons, which can be related to the formation and disintegration (rupture) of a very neutron-rich low-density region (neck) between the projectile and target.

Keywords: NUCLEAR REACTIONS ^{27}Al(^{40}Ca, X), (^{48}Ca, X), $E = 45$ MeV/nucleon; measured projectile-like fragment charge and mass distributions, light-particle velocity distributions and composite system excitation energies for incomplete fusion using FAUST array; deduced thermodynamical properties, isoscaling, effect of missing neutrons

* Corresponding author at: Laboratory of Physical Chemistry, Department of Chemistry, National and Kapodistrian University of Athens, Panepistimiopolis, Athens 15771, Greece.
E-mail addresses: soulioti@chem.uoa.gr, soulioti@comp.tamu.edu (G.A. Souliotis).
[1] Present address: C-NR, Los Alamos National Laboratory, NM 87545, USA.
[2] Present address: Physics Department, Western Michigan University, Kalamazoo, MI 49008, USA.

0375-9474/$ – see front matter
doi:10.1016/j.nuclphysa.2010.02.013

1. Introduction

The isotopic composition of nuclear reaction products provides important information on the reaction dynamics and on a possible occurrence of a phase transition in isospin-asymmetric nuclear matter [2,3], which is supposed to separate into a symmetric dense phase and an asymmetric dilute phase. It has been discussed in the literature [4] to what extent such a phase transition is generated by fluctuations of density or concentration, typically suggesting a coupling of both instability modes. The N/Z (neutron to proton ratio) degree of freedom and its equilibration was studied experimentally in detailed measurements of the isotopic distributions of emitted fragments [5–9]. Isotopically resolved data in the region of $Z = 2$–8 revealed systematic trends, which were, however, substantially affected by the decay of the excited primary fragments.

In order to investigate the thermodynamical properties of the hot multifragmentation source, the source has to be properly characterized in terms of the production mechanism and the level of equilibration. The fragment data from the reactions $^{28}Si + ^{112,124}Sn$ at projectile energy of 30 and 50 MeV/nucleon [1,10–13] provided full information (with the exception of emitted neutrons that were not detected) on the decay of thermally equilibrated hot quasi-projectiles with known mass ($A = 20$–30), charge, velocity and excitation energy. An excellent description of the dynamical properties of the reconstructed quasi-projectile, such as velocity, excitation energy and isospin-asymmetry, as well as the fragment observables such as multiplicity, charge and isotope distributions was obtained [10] using the model of deep-inelastic transfer (DIT) [14] for the early stage of collisions and the statistical multifragmentation model (SMM) [15] for the de-excitation. The contribution from non-equilibrium processes such as pre-equilibrium emission was shown to be weak [10]. The model calculation showed that the average number of neutrons not detected in the experiment was between one and two per event. Therefore, no significant distortion of the results can be expected. The observed trends of thermodynamical observables provided several correlated signals of isospin-asymmetric liquid–gas phase transition [1,13], in particular a unique signal seen in the evolution of the isovector chemical potential [1].

The present work is an extension of these studies aiming at investigating the effect of the mass of the hot multifragmenting nuclei on observed thermodynamical properties and related signals of the isospin-asymmetric liquid–gas phase transition.

2. Experiment

The experiment was performed at the Cyclotron Institute of Texas A&M University, using 45 MeV/nucleon $^{40,48}Ca$ beams delivered by the K500 superconducting cyclotron impinging on Al (2.2 mg/cm^2) target. The multidetector array FAUST [16] was employed covering forward angles between 2 and 35°, where fragments originating from the projectile-like source can be expected due to beam velocity. FAUST consists of 68 charged particle telescopes arranged in five rings. Each particle telescope consists of a 300 μm thick silicon detector followed by a 3 cm thick CsI(Tl) crystal. The angular ranges covered by the rings were chosen in order to distribute the multiplicity of detected particles evenly, thus avoiding cases where one telescope is hit simultaneously by multiple particles. In the experiment, the mass and atomic number of the detected charged particles were identified up to $Z = 8$ for the detectors in the forward rings.

The method of isotope identification uses a particle telescope technique in which the isotopes are resolved in two-dimensional ΔE–E spectra. We used a method which enables to perform the isotope identification and energy calibrations simultaneously using a minimization procedure [17,18]. In the experimental spectra, the lines for three known isotopes (typically ^1H, ^4He,

^{7}Be) are assigned and energy calibration is performed by the minimization procedure where these lines are fitted to corresponding calculated energy losses. The calibration coefficients are thus obtained as optimum values of the minimization parameters. The silicon detectors were calibrated using an alpha-source, while the empirical formula of Tassan-Got [19] was used for the energy calibration of the CsI(Tl) crystals.

3. Data analysis

Using the calibration and identification procedures described above, it was possible to identify the charged particles and to determine their energies on an event-by-event basis. For the subset of events where all detected charged particles were identified, it was possible to reconstruct the mass, charge and excitation energy of the composite system, in the same way as in the previous work [10]. The analysis was performed on the subset of events with total charge larger than that of the projectile ($Z \geqslant 21$), thus selecting events where the incomplete fusion, occurring in mid-central collisions, is the dominant contributing reaction mechanism.

3.1. Statistical decay of the hot source with mass 40–50

One of the goals of the present work was to verify the behavior observed in the reaction ^{28}Si + ^{112,124}Sn. Of special interest was the verification of the signal of the liquid–gas phase transition, obtained using isoscaling analysis in our previous work [1]. Isoscaling [20] is observed when the ratio of isotopic yields of fragments from two reactions with different isospin-asymmetry exhibits an exponential dependence on the fragment isospin-asymmetry

$$R_{21}(N, Z) = Y_2(N, Z)/Y_1(N, Z) \simeq C \exp\bigl(\beta'(N - Z)\bigr), \tag{1}$$

where the parameter β' is related, in the grand-canonical limit, to the isovector free-nucleon chemical potential, since $\beta' = \Delta(\mu_n - \mu_p)/2T$, with μ_n and μ_p the free-neutron and free-proton chemical potentials, Δ expressing the difference between the neutron-rich and the neutron-poor sources and T the common temperature.

The fragment data obtained in the reactions ^{28}Si + ^{112,124}Sn at projectile energy 30 and 50 MeV/nucleon [1,10–12] provided complete information (with the exception of emitted neutrons) on the decay of thermally equilibrated hot quasi-projectiles with known mass (A = 20–30), charge, velocity and excitation energy. A simulation employing the model of deep-inelastic transfer (DIT) [14] for the early stage of collisions and the statistical multifragmentation model (SMM) [15] for de-excitation allowed excellent description of both the dynamical properties of the reconstructed quasi-projectile such as velocity, excitation energy and isospin-asymmetry and the fragment observables such as multiplicity, charge and isotope distributions [10].

The thermodynamical properties of the quasi-projectiles undergoing statistical multifragmentation [1,10–12] were investigated in order to reveal possible signals of the phase transition. The difference of isovector chemical potentials in the two reactions $\Delta(\mu_n - \mu_p)$ was estimated using isoscaling analysis. A turning-point in the trend of the observable β'T was obtained at excitation energy of about 4 MeV/nucleon. Such a behavior can be understood as a signal of the onset of chemical separation into a dense isospin symmetric phase and a dilute isospin-asymmetric phase which reverts the decreasing trend of the free nucleon chemical potential consistent with expansion of the homogeneous system. Above the turning-point, the temperature determined using the fragment yield ratios agreed well with the kinematic temperature of protons, which can be identified as the remnants of the dilute phase (nucleon gas). Such agreement between

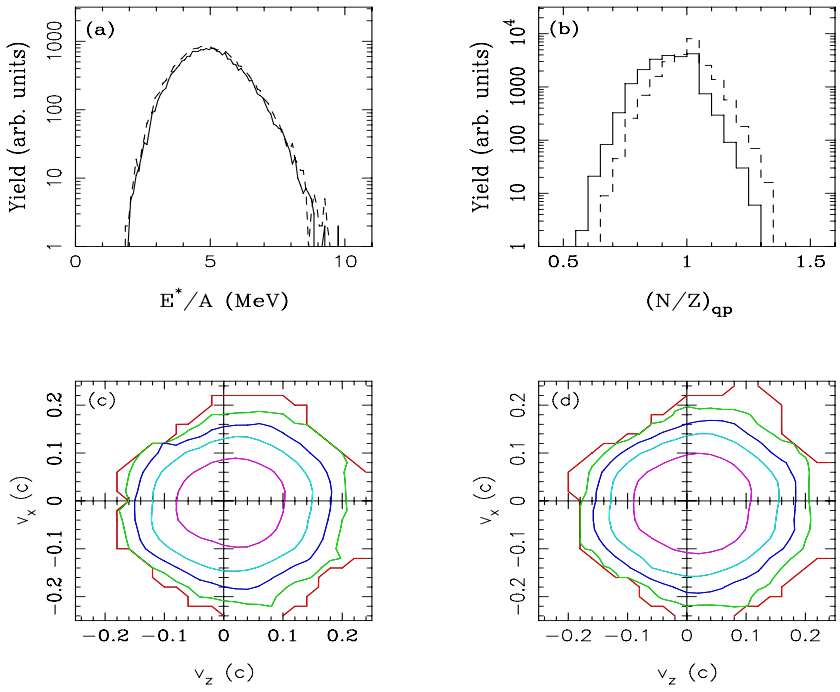

Fig. 1. (a) Excitation energy distributions of reconstructed quasi-projectiles from the reactions ^{40,48}Ca + ^{27}Al at 45 MeV/nucleon (solid line for ^{40}Ca and dashed line for ^{48}Ca), (b) N/Z-distributions of the reconstructed quasi-projectiles (solid line for ^{40}Ca and dashed line for ^{48}Ca), (c) velocity-plot of the light charged particles from the reaction ^{40}Ca + ^{27}Al at 45 MeV/nucleon, (d) velocity-plot of the light charged particles from the reaction ^{48}Ca + ^{27}Al at 45 MeV/nucleon.

the two methods of thermometry demonstrates that the grand-canonical approach describes the properties of hot nuclei undergoing multifragmentation very well. Besides isoscaling, another grand-canonical scaling was observed since the isobaric yield ratio Y(^{3}H)/Y(^{3}He) exhibited an exponential dependence on the quasi-projectile N/Z ratio. The experimental data from the reactions ^{28}Si + ^{112,124}Sn at projectile energy 30 and 50 MeV/nucleon are thus well understood in terms of a reaction mechanism where the projectile and target nuclei form a di-nuclear configuration, exchange a considerable amount of nucleons and, after re-separation, reach thermal equilibrium at different temperatures. The highly excited quasi-projectile continues to expand up to the spinodal contour.

As a first step of the analysis, the characteristics of the projectile-like nuclei, observed at forward angles, were reconstructed on an event-by-event basis. The results for the fully resolved quasi-projectiles with $Z \geqslant 21$, which are expected to originate dominantly from incomplete fusion reactions at mid-central impact parameters are shown in Fig. 1. The excitation energy distributions of the reconstructed quasi-projectiles in the reactions ^{40,48}Ca + ^{27}Al at 45 MeV/nucleon (Fig. 1(a)) are practically identical, which is somewhat surprising when taking into account that the number of missing (undetected) neutrons may differ considerably. A possible uncertainty in the evolution of neutrons can be documented also by the observed N/Z-distributions (Fig. 1(b)) which only partially reflect the initial N/Z-difference of the two projectile nuclei (amounting to 0.48), since the mean values (centroids) in the reactions ^{40,48}Ca + ^{27}Al are N/Z = 0.93 and 1.01,

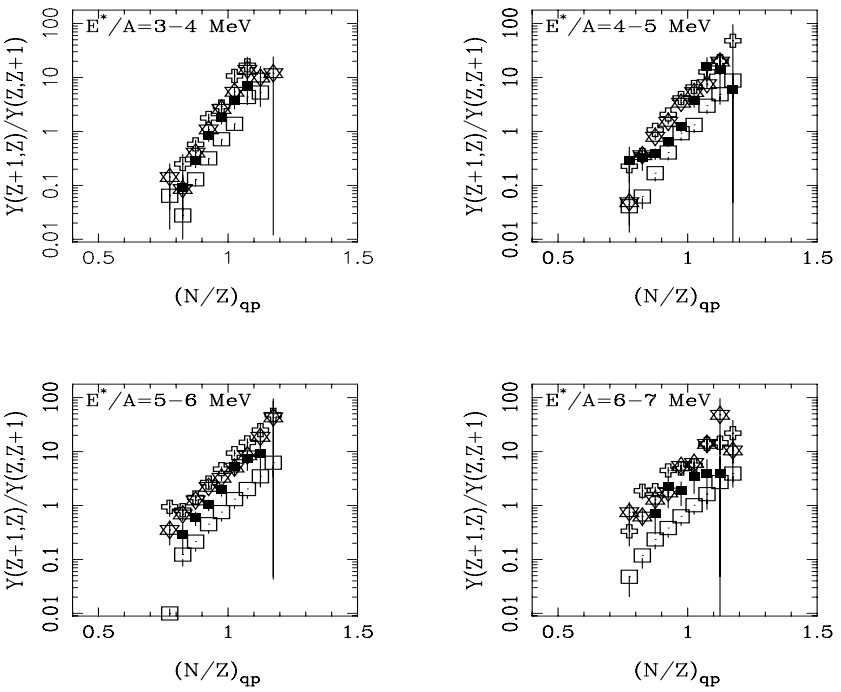

Fig. 2. Yield ratios of mirror nuclei (^{3}H/^{3}He — open squares, ^{7}Li/^{7}Be — thick crosses, ^{11}B/^{11}C — stars, ^{15}N/^{15}O — solid squares) observed in the reaction ^{48}Ca + ^{27}Al at 45 MeV/nucleon plotted for four excitation energy bins as a function of N/Z of the reconstructed projectile-like nuclei.

respectively. The velocity plots of the light charged particles in the quasi-projectile frame from these two reactions are also shown in Fig. 1 (for ^{40}Ca on panel 1(c) and for ^{48}Ca on panel 1(d)). Practically isotropic emission is observed which again implies statistical multifragmentation of the hot projectile-like nucleus. A slight suppression at the backward hemisphere is caused by the combined effect of limited angular coverage and energy thresholds of the experimental device. Using the observed characteristics of the quasi-projectile, the centrality of the observed data was estimated using the simulation, successful in describing properties of the hot multifragmenting sources formed in violent collisions in many reactions in the Fermi energy domain [21,22]. Comparison of the properties of the hot quasi-projectile source leads to the conclusion that incomplete fusion collisions at mid-central impact parameters contribute dominantly, mainly due to the narrow angular acceptance of the experimental setup around the beam direction for the reconstructed quasi-projectiles with $Z \geqslant 21$. Similar selectivity was experimentally observed in the heavy residue data from the reaction ^{124}Sn + ^{27}Al [22].

Statistical emission in the projectile-like frame is indicated also in Fig. 2. In a similar way as in the reactions ^{28}Si + ^{112,124}Sn, where the isobaric ratio ^{3}H/^{3}He exhibited an exponential (grand-canonical) scaling with the quasi-projectile N/Z, several yield ratios of mirror nuclei measured in the reaction ^{48}Ca + ^{27}Al at 45 MeV/nucleon are plotted as functions of the N/Z of the reconstructed projectile-like nuclei. Again an exponential scaling is observed, with identical slopes for all ratios within each of the excitation energy bins. The slope decreases with increasing excitation energy in an analogous way as in the reactions ^{28}Si + ^{112,124}Sn [12]. The observed grand-canonical scaling provides evidence that statistical multifragmentation is a dom-

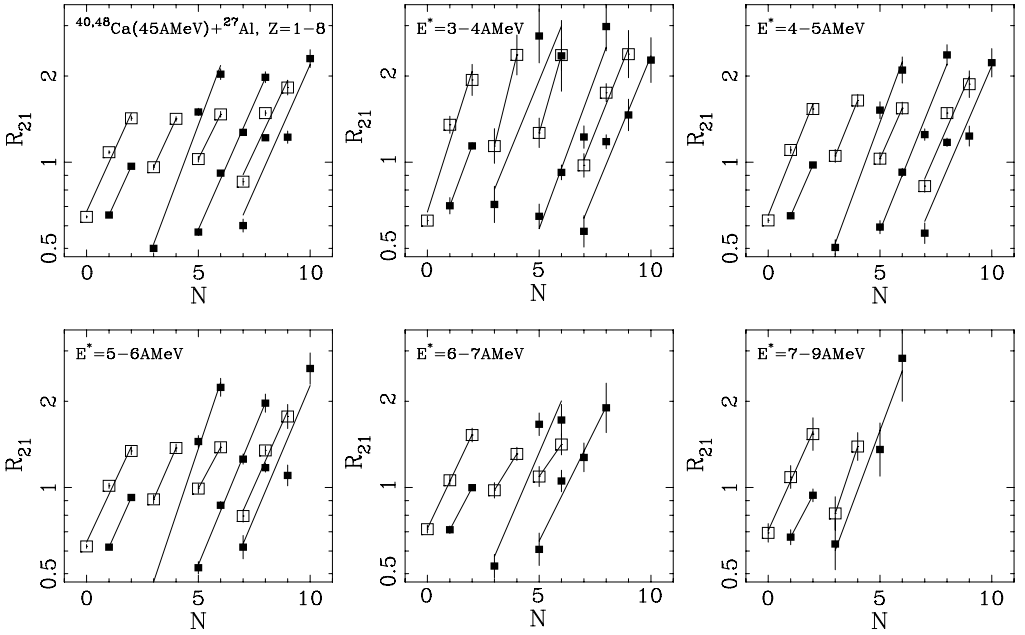

Fig. 3. Isoscaling plots, constructed for the pair of reactions ^{40,48}Ca + ^{27}Al at 45 MeV/nucleon using the identified fragments with Z = 1–8 forming the fully resolved quasi-projectiles with Z ⩾ 21. The first panel is for the full set of data, whereas the subsequent five panels refer to the indicated excitation energy bins.

inant mode of de-excitation also in the present case. It is also remarkable that essentially no effect of missing neutrons on the observed slope can be seen in this neutron-rich system which is expected to evaporate an increasing number of neutrons with increasing neutron excess of the quasi-projectile.

As in the previous work [1], the isoscaling analysis was performed also for the reactions ^{40,48}Ca + ^{27}Al at 45 MeV/nucleon. Fig. 3 shows isoscaling plots presented as a function of the fragment neutron number, constructed using the identified fragments for the fully resolved quasi-projectiles with Z ⩾ 21 for the full data set (first panel) and for five excitation energy bins (for the subsequent panels, as indicated in the figure). The observed isoscaling behavior is quite regular and the value of the isoscaling parameter (slope) decreases with excitation energy, in agreement with the previous experiment [1] and other experiments reported in the literature.

In order to estimate the evolution of the chemical potential, as in the previous work [1], one needs to estimate the system temperature. Fig. 4 shows the caloric curve obtained for the selected fully resolved data with Z ⩾ 21 using the double isotope ratio thermometer d,t/^{3,4}He (squares). Furthermore, Fig. 4 shows the comparison of the double isotope ratio thermometer d,t/^{3,4}He to another thermometer d,t/^{6,7}Li (triangles) and to the kinematic (slope) temperatures of protons, deuterons, tritons, ^{3}He and alpha particles. One can see that, unlike the previous work [13], there is no clear correspondence of any slope temperature to the double isotope ratio thermometers. Thus one needs to establish to what extent the double isotope ratio temperature of the two thermometers represents the multifragmentation temperature. A good judgment can be obtained when comparing the d,t/^{3,4}He temperature observed in the present work to the earlier results for the reactions ^{28}Si + ^{112,124}Sn [12,13]. Such a comparison shows that the caloric curves obtained in both reactions are consistent and, thus, possibly represent general properties of the multi-

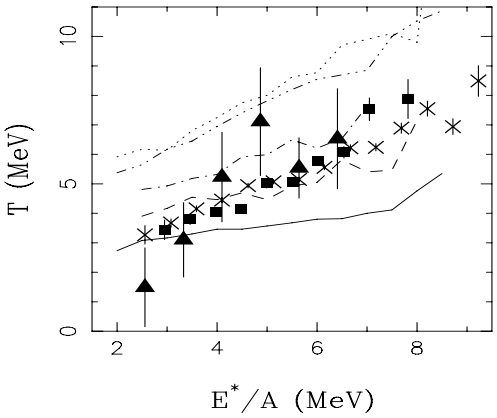

Fig. 4. Caloric curve obtained using the double isotope ratio thermometer d,t/^{3,4}He (squares), compared to the thermometer d,t/^{6,7}Li (triangles), and to the kinematic temperatures of protons, deuterons, tritons, ^{3}He and alpha particles (solid, dashed, single dot-dashed, dotted and multiple dot-dashed lines, respectively). Combined fully resolved data with $Z \geqslant 21$ from two reactions ^{40,48}Ca + ^{27}Al at 45 MeV/nucleon were used. Thin crosses show the caloric curve obtained using the thermometer d,t/^{3,4}He in the reactions ^{28}Si + ^{112,124}Sn [12].

fragmenting system. On the other hand, a similar comparison for the proton kinetic temperature shows that in the heavier system it dropped considerably, which can be explained by the onset of intense secondary emission of protons in the heavier system. Thus the mass range observed in the present work may represent an upper limit where the effect of secondary emission can be disentangled.

Moreover, since the double isotope ratio thermometers d,t/^{3,4}He and d,t/^{6,7}Li are just two of many possible thermometers, one can define a global temperature as an average value over the larger set of double isotope ratio thermometers. Such global temperature can be obtained using a graphical method developed in our previous works [23,24]. The isotopic yield ratios, corrected for mass and ground state spin, can be plotted as a function of the difference of binding energies. The resulting plots for the present data are shown in Fig. 5 for nine excitation energy bins.

The observed exponential (and thus again grand-canonical) scaling is reasonably good and one can assume that the fitted slope provides a global double isotope ratio temperature. Fig. 6(a) shows the resulting caloric curve, along with the results of the double isotope ratio thermometer d,t/^{3,4}He and the kinematic temperatures. It is remarkable to note, that there is a good correspondence between the global isotope ratio temperature and proton kinematic temperature. Both curves are relatively flat above 4 AMeV, which can be possibly interpreted as a long plateau. However, comparison with the lighter hot system in Ref. [1] shows that the value of the plateau temperature is much lower than it can be expected in multifragmentation. Especially in the case of thermometers using proton multiplicity and proton kinematic temperature such low temperature with flat behavior may be caused by increased influence of secondary de-excitation via nucleon (proton) emission. Such a mode is not dominant in the lighter system of Ref. [1], where the Fermi decay (analogous to multifragmentation) dominates [15]. Thus the proton kinematic temperature for the lighter system represents the earlier de-excitation stage, as is documented by higher values of the temperature [13] than in the present case.

The correspondence of the global isotope ratio temperature and the proton kinematic temperature can thus be explained by secondary emission. The scaling behavior in Fig. 5 is determined mainly by isotopic ratios of intermediate mass fragments up to oxygen, where the nucleon (pro-

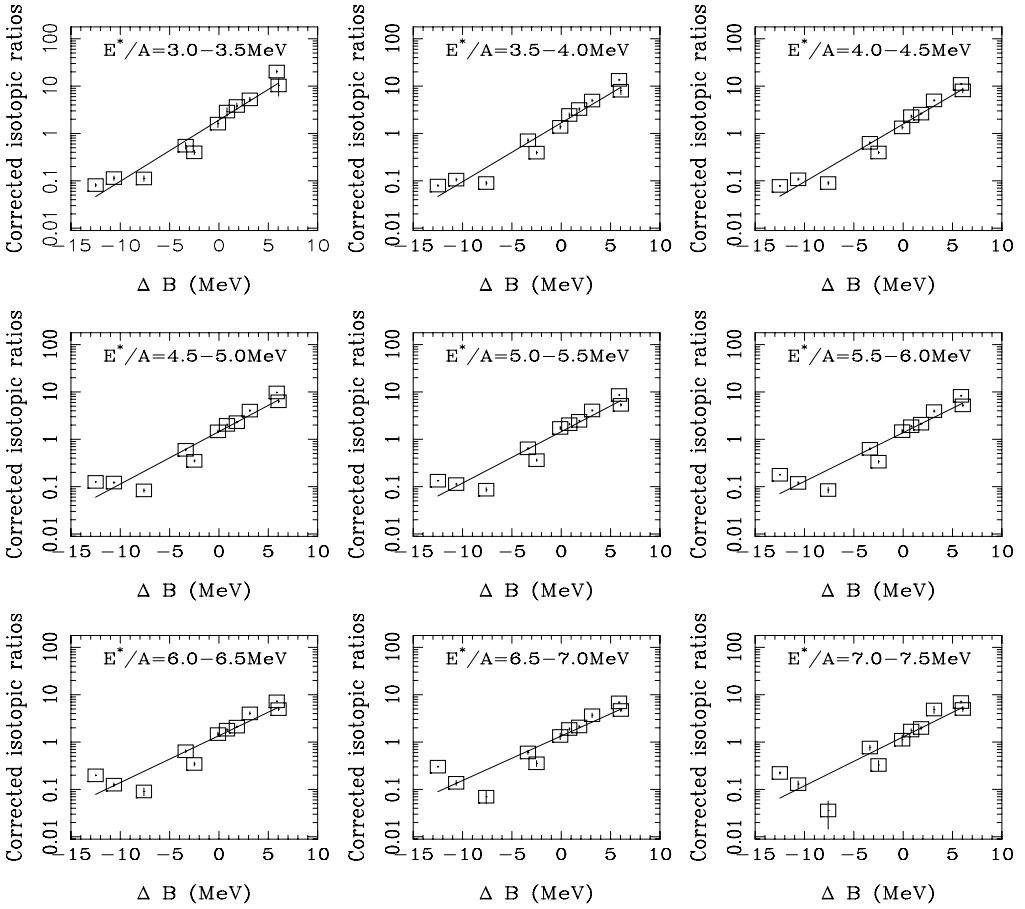

Fig. 5. Isotopic yield ratios, corrected for the mass and for the ground state spin, plotted as a function of the difference of binding energies for nine excitation energy bins.

ton) emission is an increasingly dominant mode of secondary de-excitation. Thus, it is not surprising that identical temperatures are extracted from both the Maxwellian spectra and the fragment yield ratios. Unlike proton emission, the surface emission of the isotopes used in the d,t/^{3,4}He thermometer is less probable. Therefore, their properties (as seen in their kinematic temperatures) reflect multifragmentation (volume emission) more closely. This is supported by the fact that the isotopic ratio ^{3}He/^{4}He (first point from the left in each panel of Fig. 5) does not follow the systematics. The other isotopic ratio falling out of the systematics appears to be ^{15}O/^{16}O (third from the left). Its deviation from the systematics becomes larger with increasing excitation energy, and may be caused by an increasing influence of low lying excited states. The spin degeneracy factor of these excited states can be larger than the one of the ground state which was assumed in the correction. One thus ends up with the two distinct groups of thermometers. The first group includes the thermometers based on the global isotope ratio temperature and proton kinematic temperature (and also the double isotope ratio thermometers including protons), representing the stage of secondary emission. The second group, the double isotope ratio thermometers d,t/^{3,4}He and d,t/^{6,7}Li, appear to represent an earlier stage of de-excitation, i.e.,

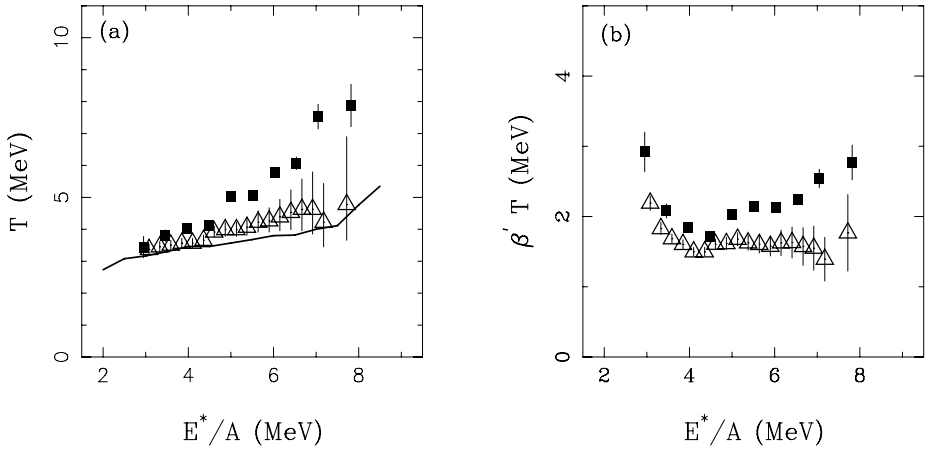

Fig. 6. (a) Caloric curve obtained using global temperature from the slopes of ΔB dependences in Fig. 5 (triangles) along with the caloric curves obtained using the double isotope ratio thermometer d,t/^{3,4}He (squares) and proton slope temperatures (line). (b) Resulting values of β'T obtained using the global (triangles) and d,t/^{3,4}He (squares) temperatures.

multifragmentation of hot nuclei. The kinematic temperatures of d, t, ^{3,4}He also appear to be consistent with the earlier stage, as was the case in the previous work [13]. However, especially for deuterons and tritons one cannot exclude a possible admixture from the later stage, either by emission or by coalescence.

In the macrocanonical limit, the product of the temperature T and isoscaling parameter β' (from Fig. 3), corresponds to the value of the isovector part of the chemical potential. The resulting values of β'T are shown in Fig. 6(b) for the d,t/^{3,4}He thermometer (squares) and the global isotope ratio temperature (from Fig. 5, triangles). In the chemical potential corresponding to the d,t/^{3,4}He thermometer, a reversion of the trend is observed at 4 MeV/nucleon, analogous to the results for the lighter system [1]. Such behavior of chemical potential was also confirmed by lattice-gas calculations [25]. The estimate of the isovector chemical potential, obtained using the thermometer representing the secondary emission, still leads to approximately constant behavior above 4 MeV/nucleon. It can be concluded that the increase of the isovector chemical potential, as documented for the d,t/^{3,4}He thermometer, is related to de-excitation of the hot multifragmenting source and signals an increasing isospin-asymmetry of the gas phase in the isospin-asymmetric liquid–gas phase transition [1]. Furthermore, one needs to take into account that secondary emission influences also the value of the isoscaling parameter. The work in Ref. [26] showed that such influence is not significant for the lighter system ($A \simeq 25$), but for the systems with $A \simeq 50$ (as in the present case) secondary emission and wide initial isotopic distributions from the dynamical stage of the collision result in higher values of the isoscaling parameters, and such trend weakens with increasing excitation energy. Thus the actual dependence may have an even deeper minimum since the effect of secondary emission tends to flatten it.

In general, one can conclude that the trends observed in the lighter quasi-projectiles in the reactions ^{28}Si + ^{112,124}Sn [1,12,13] were confirmed in the reactions ^{40,48}Ca + ^{27}Al at 45 MeV/nucleon for projectile-like nuclei with mass about twice that of the former. Moreover, it has been shown that the properties of the hot systems, as reflected by the fragment observables, become still more distorted by secondary emission with increasing mass.

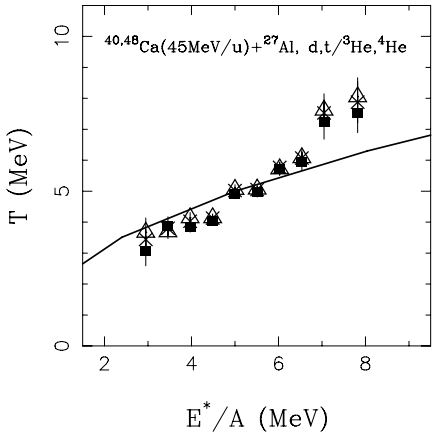

Fig. 7. Caloric curves obtained using the double isotope ratio thermometer d,t/^{3,4}He (^{40}Ca + ^{27}Al — squares, ^{48}Ca + ^{27}Al — triangles, combined data — crosses, line — theoretical dependence from Ref. [27]).

3.2. Missing neutrons — statistical or dynamical emission?

Specifically for the neutron-rich ^{48}Ca projectile, the effect of missing (undetected) neutrons must be considered. In the earlier works, it was established using successful simulations for the reactions ^{28}Si + ^{112,124}Sn that the losses due to neutron emission represent a relatively small part of the system [10]. The isospin equilibration was not complete and thus the neutron-rich target did not result in a comparably neutron-rich quasi-projectile. The effect of missing neutrons was examined using isoscaling plots expressed for sets of identical quasi-projectiles from two reactions [1]. No dependence was observed which could be attributed to the influence of missing neutrons. It was also observed that the shape of the caloric curve did not depend on the N/Z of the quasi-projectile.

In the case of the reactions ^{40,48}Ca + ^{27}Al, even when assuming an incomplete fusion scenario, one has to expect that there will be a considerable difference in neutron excess of the hot systems in the two reactions (seven neutrons according to the simulation). In this context, it is remarkable that the caloric curves, expressed as a function of excitation energy obtained by charged particle calorimetry, are almost identical in both reactions, despite the expected significant difference of total excitation energy after including the missing neutrons. Fig. 7 shows the caloric curves obtained using the double isotope ratio thermometer d,t/^{3,4}He for the reactions ^{40,48}Ca + ^{27}Al, along with the theoretical line from Ref. [27]. There is a little difference observed between the two reactions. Especially, there is no shift which could be attributed to the difference of true excitation energies, which could exceed 1 MeV/nucleon, due to a different number of emitted neutrons in the simulation (up to seven). The experimental caloric curves agree well with the theoretical dependence [27], representing temperatures where the isolated system with given excitation energy enters the spinodal contour, thus confirming the conclusion that, as in the reactions ^{28}Si + ^{112,124}Sn, the d,t/^{3,4}He thermometer represents multifragmentation of the hot equilibrated source.

Complementary to the caloric curves, also the trends of the yield ratios of mirror nuclei were compared. In Fig. 8 are shown the trends of the yield ratio of the mirror nuclei ^{3}H and ^{3}He for the two reactions ^{40,48}Ca + ^{27}Al as a function of the N/Z of the reconstructed quasi-projectile and the two dependences are identical for all four excitation energy bins. Similar behavior is observed

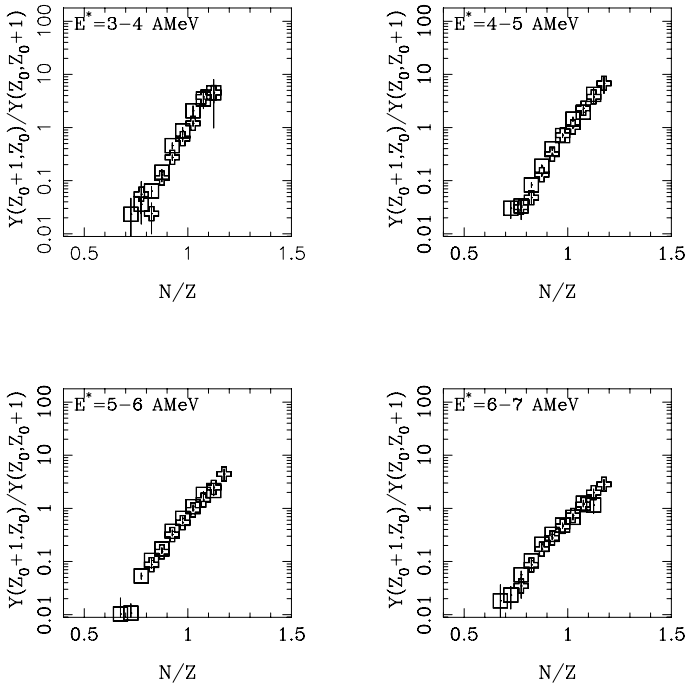

Fig. 8. Trends of the yield ratio of the mirror nuclei ^{3}H and ^{3}He for two reactions ^{40,48}Ca + ^{27}Al in four excitation energy bins plotted as a function of the N/Z of the reconstructed quasi-projectile.

also for the other three yield ratios of the mirror nuclei shown in Fig. 2. This behavior further documents that indeed the fragment yield ratios, which are used also to determine the double isotope ratio temperature, exhibit identical dependence on N/Z of the quasi-projectile, independent of the nominal neutron excess. Furthermore, the ratios of yields of specific isotopes in two reactions (isoscaling behavior) were verified using the subsets of quasi-projectiles corresponding to selected N/Z-bins. The observed slopes, representing the difference of chemical potentials, were consistent with zero, within statistical errors, so again the insensitivity to neutron excess was confirmed. Thermodynamical observables (see Figs. 1(a), 2, 7 and 8) thus, remarkably, do not exhibit sensitivity to the number of missing (undetected) neutrons in the two reactions.

As a possible explanation, one may assume that the apparent excitation energy, reconstructed using the observed charged particles, is close to the true excitation energy of the hot equilibrated source, and the excess neutrons in the neutron-rich case are not part of the equilibrated source, due to dynamical emission taking place prior to equilibration. Such explanation is consistent with the almost identical experimental excitation energy distributions shown in Fig. 1(a) for the two reactions ^{40,48}Ca + ^{27}Al and is also supported by the lack of the effect of missing neutrons on the scaling shown in Fig. 2 in the neutron-rich reaction ^{48}Ca + ^{27}Al. Dynamical emission of neutron-rich charged particles at mid-velocity was reported in recent years [28] and interpreted as caused by the formation of a neutron-rich neck. Such scenario may provide an explanation also in the present case, with the notable difference that the neck structure may be formed almost exclusively by neutrons. In the present case the low-density region between the projectile and the target is expected to be very neutron-rich [29], since the nuclear equation of state for subsaturation densities provides stable solutions only outside of the spinodal region and thus at

very asymmetric N/Z ratios. A behavior consistent with the present case was reported recently [30] in incomplete fusion reactions, where an isospin-dependent component of excitation energy was necessary to explain the production of neutron-rich fragmentation products. Such behavior is consistent with rupture of the neck structure formed mostly by neutrons in the region between the hot and cold pre-fragments during the dynamical stage. Unlike the cases where signatures of neck formation were reported in symmetric damped collisions of massive nuclei [28], in the present case the alternative explanation due to the Coulomb force from the massive external charge [31] may be excluded. The remaining charge, especially in the incomplete fusion reactions, is rather small, and the observed trends may be attributed solely to the effect of the nuclear mean field.

4. Summary and conclusions

In summary, a signal of isospin-asymmetric phase transition in the evolution of the chemical potential was observed in the multifragmentation of hot quasi-projectiles in the reactions $^{40,48}\mathrm{Ca} + {}^{27}\mathrm{Al}$ confirming an analogous observation in lighter quasi-projectiles in the reactions $^{28}\mathrm{Si} + {}^{112,124}\mathrm{Sn}$ [1]. However, with increasing mass, the properties of the hot systems become increasingly influenced by secondary emission. Thermodynamical observables exhibit no sensitivity to the different number of missing neutrons due to variation of neutron excess of the hot systems in the two reactions $^{40,48}\mathrm{Ca} + {}^{27}\mathrm{Al}$, thus, possibly providing a signal of dynamical emission of neutrons, which may be related to the formation of a neutron-rich low-density region (neck) between the projectile and target.

Acknowledgements

The authors wish to thank the staff of the Texas A&M Cyclotron facility for the excellent beam quality. This work was supported by the US Department of Energy under contract DE-FG03-93ER40773, by the Welch Foundation under contract A-1266, by the Slovak Scientific Grant Agency under contracts VEGA-2/5098/25 and VEGA-2/0073/08, by the Slovak Research and Development Agency under Contract No. SK-CN-00706, through the Agreement of Scientific Cooperation between China and Slovakia by the Ministry of Sciences and Technology and the Major State Basic Research Development Program (973 program) under Contract No. 2007CB815004, the National Natural Science Foundation of China under Contract Nos. 10775167 and 10979074, and the Shanghai Development Foundation for Science and Technology under Contract No. 09JC1416800.

References

[1] M. Veselsky, G.A. Souliotis, S.J. Yennello, Phys. Rev. C 69 (2004) 031602(R).
[2] H. Müller, B.D. Serot, Phys. Rev. C 52 (1995) 2072.
[3] V.M. Kolomietz, et al., Phys. Rev. C 64 (2001) 024315.
[4] B.-A. Li, C. Ko, Nucl. Phys. A 618 (1997) 498;
V. Baran, et al., Phys. Rev. Lett. 86 (2001) 4492;
M. Colonna, et al., Phys. Rev. Lett. 88 (2002) 122701;
J. Margueron, P. Chomaz, Phys. Rev. C 67 (2003) 041602(R).
[5] S.J. Yennello, et al., Phys. Lett. B 321 (1994) 14.
[6] H. Johnston, et al., Phys. Lett. B 371 (1996) 186.
[7] E. Ramakrishnan, et al., Phys. Rev. C 57 (1998) 1803.
[8] R. Laforest, et al., Phys. Rev. C 59 (1999) 2567.
[9] H.S. Xu, et al., Phys. Rev. Lett. 85 (2000) 716.

[10] M. Veselsky, et al., Phys. Rev. C 62 (2000) 064613.
[11] M. Veselsky, et al., Phys. Rev. C 62 (2000) 041605(R).
[12] M. Veselsky, et al., Phys. Lett. B 497 (2001) 1.
[13] M. Veselsky, S.J. Yennello, Nucl. Phys. A 749 (2005) 114c.
[14] L. Tassan-Got, C. Stéfan, Nucl. Phys. A 524 (1991) 121.
[15] J.P. Bondorf, et al., Phys. Rep. 257 (1995) 133.
[16] F. Gimeno-Nogues, et al., Nucl. Instrum. Meth. A 399 (1997) 94.
[17] M. Veselsky, et al. Progress in Research, 2000–2001, Cyclotron Institute, Texas A&M University, College Station, 2001, p. V-13.
[18] A.L. Keksis, Ph.D. thesis, Cyclotron Institute, Texas A&M University, 2007.
[19] L. Tassan-Got, Nucl. Instrum. Meth. B 194 (2002) 503.
[20] M.B. Tsang, et al., Phys. Rev. Lett. 86 (2001) 5023.
[21] M. Veselsky, Nucl. Phys. A 705 (2002) 193.
[22] M. Veselsky, et al., Nucl. Phys. A 724 (2003) 431.
[23] M. Veselsky, G.A. Souliotis, S.J. Yennello, in: Proc. 5th Int. Conf. DANF-2001, Casta-Papiernicka, Slovakia, 2001, World Scientific, 2002, p. 461, arXiv.org:nucl-ex/0112007.
[24] D.V. Shetty, et al., Phys. Rev. C 68 (2003) 054605.
[25] Y.G. Ma, et al., Phys. Rev. C 69 (2004) 064610.
[26] M. Veselsky, Phys. Rev. C 74 (2006) 054611.
[27] M. Veselsky, Int. J. Mod. Phys. E 17 (2008) 1883, arXiv.org:nucl-th/0703077.
[28] G. Casini, et al., Phys. Rev. Lett. 71 (1993) 2567;
C.P. Montoya, et al., Phys. Rev. Lett. 73 (1994) 3070;
J.F. Dempsey, et al., Phys. Rev. C 54 (1996) 1710.
[29] M. Di Toro, A. Olmi, R. Roy, Eur. Phys. J. A 30 (2006) 65.
[30] M. Veselsky, G.A. Souliotis, Nucl. Phys. A 781 (2007) 521.
[31] M. Jandel, et al., J. Phys. G 31 (2005) 29.